

# Mode Conversion in Circular Waveguides

By E. R. NAGELBERG and J. SHEFER

(Manuscript received May 14, 1965)

*Mode conversion from  $TE_{11}$  to  $TM_{11}$  modes in circular waveguides is investigated. It is found that an iris placed across the waveguide or an abrupt change in guide radius (step) will produce a wide range of mode conversion coefficients which can be used in most dual-mode feedhorn applications. The step discontinuity is found to produce relatively constant mode conversion over a wide band of frequencies.*

## I. INTRODUCTION

In order to obtain optimum illumination at the aperture of a dual-mode conical horn,<sup>1</sup> as in the open cassegrain antenna,<sup>2</sup> it is necessary to control the relative amplitudes and phases of the  $TE_{11}$  and  $TM_{11}$  modes. The mode combination is established (considering the antenna as a transmitter) by exciting the dominant mode ( $TE_{11}$ ) in the circular waveguide that feeds the horn, and converting a part of that signal to propagate in the  $TM_{11}$  mode by introducing suitable transmission line discontinuities in the vicinity of the waveguide to cone transition (Fig. 1). The general requirement that a discontinuity be suitable for mode conversion as described above is that it perturb the incident transverse electric field in such a way as to produce a component of electric field in the direction of propagation. This may be done by introducing a conducting surface transverse to the direction of propagation, in which case the coupling arises directly from the fact that the component of electric field tangent to the surface must vanish.

To be generally useful, the mode conversion configuration must provide controlled mode conversion over a useful band of frequencies without introducing significant reflection of the input  $TE_{11}$  mode. It is further required that the converter discontinuity be circularly symmetric, both to prevent excitation of unwanted modes and to permit operation of the device for signals of arbitrary polarization.

Three basic schemes are possible, the iris, the groove, and the step, each of which is shown in Fig. 2.

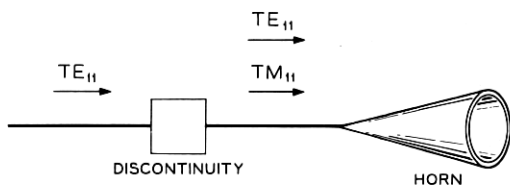


Fig. 1 — Horn and mode converter discontinuity.

It has been found that each of the configurations in Fig. 2 can provide adequate mode conversion with suitable adjustment. However, in cases (a) and (b), a single discontinuity excites both backward and forward propagating  $TM_{11}$  modes. This backward wave, after reflection from a transition (see Section 2.2) from standard to oversized waveguide, combines with the forward traveling wave with a relative phase which is highly frequency dependent, thus making a transition and single iris a frequency sensitive system. In addition, configuration (b) has an intrinsic dispersion due to resonance in the groove itself.

If the diameter of the input waveguide is chosen small enough so that it will not support a  $TM_{11}$  mode over the frequency band, configuration (c) behaves very well over a wide band. Such a discontinuity was used by Potter<sup>1</sup> in early experiments with dual-mode horn excitation.

## II. THEORETICAL ASPECTS OF MODE CONVERSION

### 2.1 General Considerations.

The  $TE_{11} \rightarrow TM_{11}$  mode conversion may be accomplished by introducing a circularly symmetric perturbation into a section of circular waveguide preceding the horn throat. Assume that the effect of this perturbation is to produce, at  $z = 0$ , a longitudinal component of electric

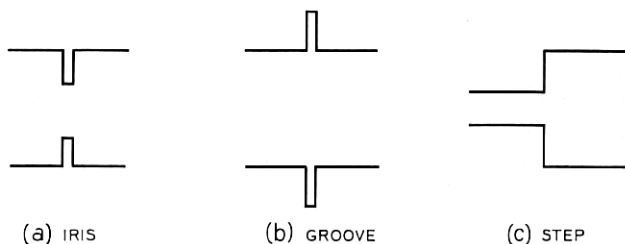


Fig. 2 — Three types of mode converters.

field with  $\cos \varphi$  symmetry. A typical section along the  $z$ -axis will be as shown in Fig. 3. If the incident transverse electric field is given by

$$\mathbf{E}_t^{(\text{inc})} = E_0 \left[ \mathbf{e}_\rho \frac{J_1(\gamma\rho/a)}{\rho/a} \cos \varphi - \mathbf{e}_\varphi J_1'(\gamma\rho/a) \sin \varphi \right] \exp(-j\beta_{\text{TE}}z) \quad (1)$$

where  $\gamma = 1.841$ , then interaction at the obstacle will produce a longitudinal electric field at  $z = 0$  of the form,

$$E_z(z = 0) = E_0 f(\rho/a) \cos \varphi \quad (2)$$

where  $f(\rho/a)$  will, of course, depend on the geometry. The resulting  $\text{TM}_{11}$  mode propagating in the  $+z$  direction will then have the following components:

$$\begin{aligned} E_z^{\text{TM}} &= A J_1(\chi\rho/a) \cos \varphi \exp(-j\beta_{\text{TM}}z) \\ E_\rho^{\text{TM}} &= \frac{-j\beta_{\text{TM}}a}{\chi} A J_1'(\chi\rho/a) \cos \varphi \exp(-j\beta_{\text{TM}}z) \\ E_\varphi^{\text{TM}} &= \frac{j\beta_{\text{TM}}a}{\chi^2} \frac{A J_1(\chi\rho/a)}{\rho/a} \sin \varphi \exp(-j\beta_{\text{TM}}z) \end{aligned} \quad (3)$$

where

$$\chi = 3.832$$

and

$$A = \frac{2E_0}{[J_0(\chi)]^2} \int_0^1 \zeta f(\zeta) J_1(\chi\zeta) d\zeta \quad (4)$$

where  $f(\zeta)$  describes the radial dependence of  $E_z$ , as in (2). A convenient parameter, for both design and measurement purposes, is the ratio of magnitudes of the  $\rho$  components of the  $\text{TM}_{11}$  and  $\text{TE}_{11}$  electric fields, evaluated at  $\rho = a$ ,  $\varphi = 0$ . This will be referred to as the conversion

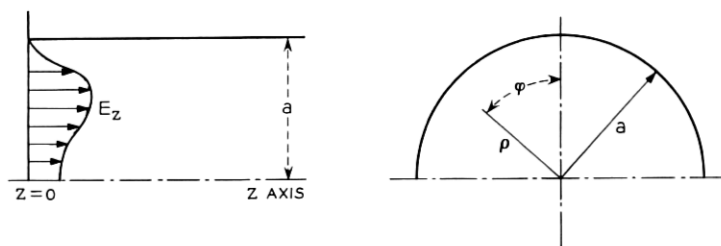


Fig. 3—Effect of perturbation is to produce a longitudinal electric field at  $z = 0$ .

coefficient and is given by

$$\begin{aligned}
 C &= \left| \frac{E_{\rho}^{\text{TM}}}{E_{\rho}^{\text{TE}}} \right| (\rho = a, \varphi = 0) \\
 &= \left| \frac{2\beta_{\text{TM}} a J_1'(\chi)}{\chi J_1(\gamma) [J_0(\chi)]^2} \int_0^1 \xi f(\xi) J_1(\chi \xi) d\xi \right| \quad (5) \\
 &= 2.2\beta_{\text{TM}} a \left| \int_0^1 \xi f(\xi) J_1(\chi \xi) d\xi \right|
 \end{aligned}$$

which, in principle, may be calculated once the longitudinal electric field is known.

In the design of dual-mode conical horns, it is necessary to specify conditions at the radiating aperture, since it is the field distribution at this cross section which determines the feed characteristics. If we let the subscript 2 denote conditions at the aperture and the subscript 1 denote conditions at the cross section where conversion occurs, then the respective coefficients are related by

$$\frac{C_2}{C_1} = \frac{f}{f_c^{\text{TM}}} \left\{ \left[ \left( \frac{f}{f_c^{\text{TM}}} \right)^2 - 1 \right] \left[ \left( \frac{f}{f_c^{\text{TM}}} \right)^2 - 0.23 \right] \right\}^{-1} \quad (6)$$

where  $f_c^{\text{TM}}$  is the  $\text{TM}_{11}$  cutoff frequency at the cross section where conversion occurs. The relationship of (6) is given in Fig. 4. To derive (6), the following assumptions are made:

- (1.) The power transmitted in each mode is constant, i.e., the horn is lossless and no further conversion occurs.
- (2.) The transverse electromagnetic fields at any cross section of a

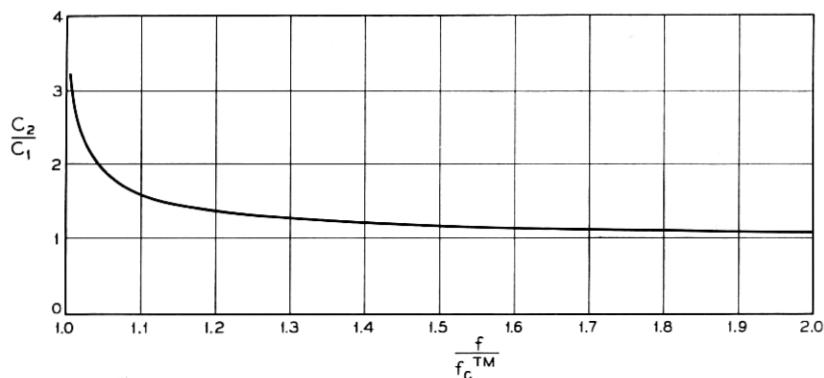


Fig. 4—A graph of ratio of coefficients at horn aperture and converter.

narrow angle conical horn are approximately the same as in a circular waveguide with the same radius as the cross section.

(3.) The aperture diameter is much larger than the cutoff diameter for the  $TM_{11}$  mode, so that at the aperture the guide wavelengths of both modes are approximately equal to the free space wavelength.

Although the conversion coefficient as defined above refers only to the relative amplitudes of the two modes, one should recognize that it is equally important that their relative phases at the horn aperture be kept within tolerable limits over the prescribed frequency band. If we assume that the relative phase at the converter discontinuity is frequency independent, then the error is due to the difference in electrical length for the two modes as they propagate through the horn.

Consider the conical horn shown in Fig. 5, which has an aperture radius  $r_0$  and half angle  $\alpha$ . It can be shown that the phase shift between the converter and aperture cross sections for a single mode is given approximately by

$$\theta_{12} = \frac{1}{\kappa_2 p} \sqrt{1 - \kappa_2^2} - \kappa_2 \cos^{-1} \kappa_2 - \frac{1}{\kappa_1 p} \sqrt{1 - \kappa_1^2} - \kappa_1 \cos^{-1} \kappa_1 \quad (6a)$$

where

$$\kappa_{1,2} = \frac{2\pi z_{1,2}}{\lambda_0 p}$$

and  $p$  is equal to  $\sin \alpha/1.84$  and  $\sin \alpha/3.83$  for the  $TE_{11}$  and  $TM_{11}$  modes respectively.

Fig. 6 shows the result of calculating the differential phase shift  $\theta_{12}^{TE} - \theta_{12}^{TM}$  at the aperture of a horn with  $r_0 = 12\lambda_0$  and  $\alpha = 3.25^\circ$ . The frequency range is 3.7–4.2 mc and conversion is assumed to take place at that cross section with radius equal to 1.5 times the cutoff radius for the  $TM_{11}$  mode at 3.7 mc.

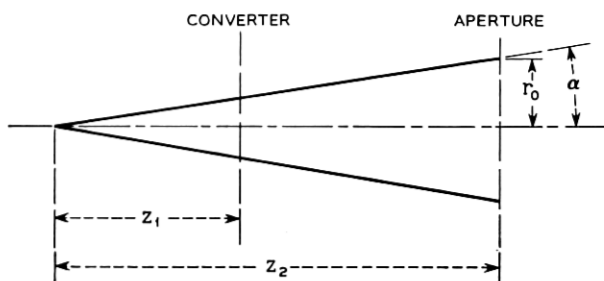


Fig. 5—Conical horn.

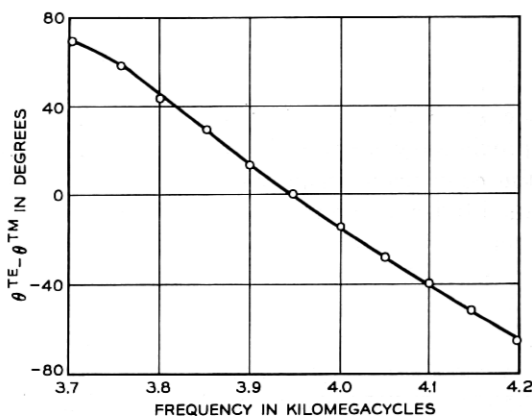


Fig. 6—Differential phase shift as a function of frequency for  $\tau_0 = 12\lambda_0$  and  $\alpha = 3.25^\circ$ .

## 2.2 Mode Conversion at an Iris

To demonstrate the application of these formulas, we consider the example of mode conversion at an iris in an oversized circular waveguide, as shown in Fig. 7. The purpose of the standard input circular waveguide and subsequent transition is to prevent the uncontrolled excitation of a  $TM_{11}$  mode at the input of the system.

In order to calculate the conversion coefficient it is necessary to have an expression for the longitudinal component of electric field at  $z = 0$ . This may be determined, in principle, by solving the interior boundary value problem associated with the iris, i.e. by obtaining a solution to Maxwell's equations which has the following characteristics:

(1.) The component of electric field tangent to the waveguide, transition, and iris walls must vanish.

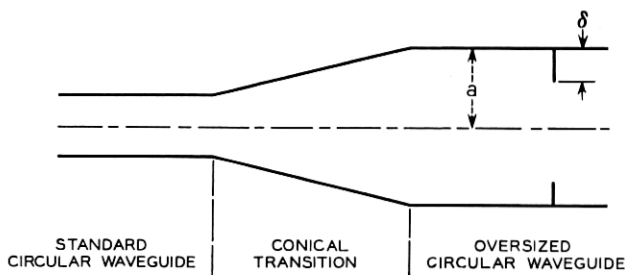


Fig. 7—Mode conversion at an iris.

(2.) At  $z = +\infty$  the field should consist of a linear combination of  $TE_{11}$  and  $TM_{11}$  modes propagating in the forward direction; at  $z = -\infty$  the field should consist of a given  $TE_{11}$  mode propagating in the forward direction and a reflected  $TE_{11}$  mode propagating back toward the source.

(3.) The singularity at the edge of the iris should be such that the energy in any finite element of volume is finite.

Although the exact solution to the problem as stated is prohibitively complex, it is possible to make certain simplifying assumptions and still obtain useful information, which is in agreement with observation, particularly with respect to the variation of mode conversion with iris size and frequency. We approach the problem within the framework of perturbation theory, and assume that the incident  $TE_{11}$  wave is unperturbed at distances far from the iris, but is distorted at the iris walls in such a way as to produce a longitudinal component of electric field. An analogous two-dimensional electrostatics problem is the case of a uniform electric field terminated by a perfectly conducting plane with a thin protrusion, as shown in Fig. 8. If  $E_0$  is the magnitude of the uniform field, then the  $x$  component of electric field in the plane  $x = 0$  is given by

$$\begin{aligned}
 E_x &= \frac{E_0 y}{\sqrt{y^2 - \delta^2}} & x = 0+, & \quad 0 \leq y < \delta \\
 E_x &= \frac{-E_0 y}{\sqrt{y^2 - \delta^2}} & x = 0-, & \quad 0 \leq y < \delta \\
 E_x &= 0 & x = 0, & \quad y > \delta.
 \end{aligned}
 \tag{7}$$

We are motivated, by analogy, to assume that the longitudinal electric field at the iris is given by a function of the form

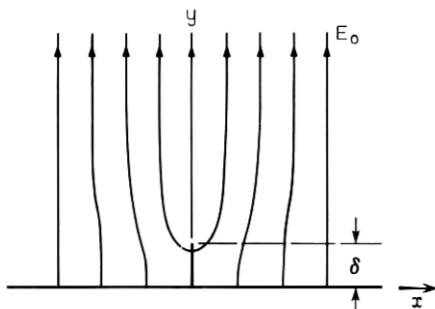


Fig. 8—A uniform electrostatic field terminated by a perfectly conducting plane with a thin protrusion.

$$\begin{aligned}
 E_z(\rho, \varphi, z = 0+) &= E_\rho^{\text{TE}}(\rho=a) \left( \frac{a-\rho}{\delta} \right) g(1-\rho/a) \\
 &= E_0 \cos \varphi \left( \frac{a-\rho}{\delta} \right) g \left( \frac{a-\rho}{\delta} \right) \\
 & \qquad \qquad \qquad a \geq \rho > a - \delta \quad (8)
 \end{aligned}$$

$$\begin{aligned}
 E_z(\rho, \varphi, z = 0-) &= -E_0 \cos \varphi \left( \frac{a-\rho}{\delta} \right) g \left( \frac{a-\rho}{\delta} \right) \\
 & \qquad \qquad \qquad a \geq \rho > a - \delta
 \end{aligned}$$

$$\begin{aligned}
 E_z(\rho, \varphi, z = 0\pm) &= 0 \\
 & \qquad \qquad \qquad a - \delta > \rho \geq 0.
 \end{aligned}$$

Note that the uniform electric field of the electrostatic problem is replaced by the unperturbed  $\rho$  component of electric field of the  $\text{TE}_{11}$  mode, evaluated at  $\rho = a$ . In addition, an undetermined function  $g(\xi)$  has been introduced to account for the singularity at  $\rho = a - \delta$ . This function may be expected to have the general behavior indicated in Fig. 9, and must be square integrable on  $(0,1)$ .

It was noted earlier that two  $\text{TM}_{11}$  waves, with equal amplitudes, propagate in opposite directions away from the iris. The forward wave will travel unperturbed; however, the backward wave is totally reflected from the transition since, by assumption, the waveguide to the left of the transition will not support a  $\text{TM}_{11}$  mode. This reflected wave will then combine with the forward wave excited at the iris. Since the reflected wave arrives back at the iris with a phase which is highly fre-

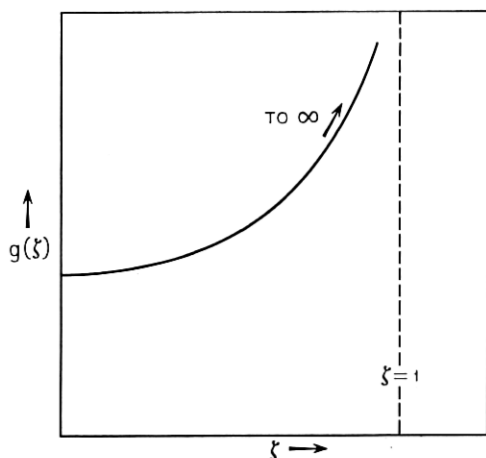


Fig. 9—Expected behavior of the function  $g(\xi)$ .



quency dependent, the amplitude of the sum varies rapidly with frequency.

Consider the wave initially excited in the forward direction. In order to calculate the conversion coefficient  $C_0$ , if only this wave were present, substitute the expression for  $E_z(\rho, \varphi, z = 0+)$  as given in (8), into (5). This result is relevant even when the backward wave is taken into account, since  $2C_0(\delta/a, ka)$  will then give the envelope of the combination as the frequency is varied. Under the assumption of small conversion

$$C_0 \approx \frac{2\alpha\beta_{TM}a}{J_1(\gamma)} \left(\frac{\delta}{a}\right)^2 + O\left[\left(\frac{\delta}{a}\right)^3\right] \tag{9}$$

$$\approx \frac{2\alpha ka}{J_1(\gamma)} \frac{\lambda}{\lambda_g^{TM}} \left(\frac{\delta}{a}\right)^2$$

where  $\alpha$  is the second moment of the singularity function  $g(\zeta)$ ,

$$\alpha = \int_0^1 \zeta^2 g(\zeta) d\zeta. \tag{10}$$

The value of  $\alpha$ , assuming a square root singularity

$$g(\zeta) = \frac{1}{\sqrt{1 - \zeta^2}} \tag{11}$$

as in the electrostatic case, would be  $\alpha = \pi/4$ , giving the "quasi-static" expression for the conversion coefficient

$$C_0 \approx \frac{\pi ka}{2J_1(\gamma)} \frac{\lambda}{\lambda_g^{TM}} \left(\frac{\delta}{a}\right)^2. \tag{12}$$

### 2.3 Mode Conversion by a Step

We now consider the problem of mode conversion at a simple discontinuity from a standard size waveguide, in which only the  $TE_{11}$  mode can propagate, to one which is oversized to support a  $TM_{11}$  mode as well. The configuration is shown in Fig. 10.

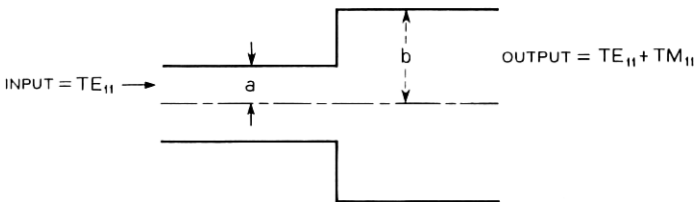


Fig. 10 — Mode conversion at a step.

The approach we use to determine the conversion coefficient in this case is somewhat different than the quasi-static approximation used for the iris. It may be shown that a knowledge of the transverse electric field at a cross section of waveguide uniquely determines the amplitudes of the TE and TM modes which comprise this field. In the present problem this implies that a knowledge of  $E_t(\rho, \varphi)$  at  $z = 0$  would permit the calculation, in principle, of the conversion coefficient for the step discontinuity. We have observed experimentally that the input standing wave ratio is very low for frequencies more than 5 per cent above the  $TM_{11}$  mode cut-off frequency for the oversized waveguide. This motivates the "perfect match" approximation for mode conversion by a step discontinuity, in which we calculate the modes propagating to the right by assuming that at  $z = 0$  the transverse field in the common aperture is that due only to the unperturbed incident  $TE_{11}$  mode. Thus at  $z = 0$

$$\begin{aligned} E_\rho &= E_0 a / \gamma \rho J_1(\gamma \rho / a) \cos \varphi & 0 \leq \rho \leq a \\ &= 0 & a < \rho \leq b \\ E_\varphi &= -E_0 J_1'(\gamma \rho / a) \sin \varphi & 0 \leq \rho \leq a \\ &= 0 & a < \rho \leq b. \end{aligned} \quad (13)$$

The components of the  $TM_{11}$  electric field to the right of the discontinuity will be given by

$$\begin{aligned} E_z^{TM} &= A J_1(\chi \rho / b) \cos \varphi \exp(-j\beta_{TM} z) \\ E_\rho^{TM} &= \frac{-j\beta_{TM} b}{\chi} A J_1'(\chi \rho / b) \cos \varphi \exp(-j\beta_{TM} z) \\ E_\varphi^{TM} &= \frac{+j\beta_{TM} b^2}{\chi^2 \rho} A J_1(\chi \rho / b) \sin \varphi \exp(-j\beta_{TM} z) \end{aligned} \quad (14)$$

where  $A$  is related to the transverse electric field at  $z = 0$  by the expression

$$A^2 = -\frac{2\chi^2}{\beta_{TM}^2 \pi b^4} \int_{\rho=0}^a \int_{\varphi=0}^{2\pi} \mathbf{E}_t \cdot \mathbf{E}_t^{TM} \rho d\rho d\varphi \quad (15)$$

where  $\mathbf{E}_t$  is given in (13) and  $\mathbf{E}_t^{TM}$  in (14), evaluated at  $z = 0$ . The calculation may be further simplified by assuming that

$$b = a(1 + \epsilon) \quad (16)$$

where  $\epsilon \ll 1$ , which is a case of practical interest. Under this additional approximation the conversion coefficient may be shown to be

$$C = 2 \frac{b-a}{a} + O \left[ \left( \frac{b-a}{a} \right)^2 \right] \quad (17)$$

for the perfect match case.

### III. METHOD OF MEASUREMENT

The  $TM_{11}$  mode propagating in the positive  $z$  direction will produce a spatial beat with the  $TE_{11}$  mode propagating with a different phase velocity, the net effect being a standing wave. A moving probe is used to measure the standing wave ratio, which in turn is directly related to the amplitude ratio of the two modes.

Suppose the radial electric field components of the two modes at  $\rho = a$  and  $\varphi = 0$  in Fig. 11 are given by

$$\begin{aligned} E_{\rho}^{TE} &= A \exp(-j\beta_{TE}z) \\ E_{\rho}^{TM} &= B \exp(-j\beta_{TM}z) \end{aligned} \quad (18)$$

then the current of a square law detector with an electric probe at  $\rho = a$ ,  $\varphi = 0$  is given by

$$I \approx |\exp(-j\beta_{TE}z) + C \exp(j\phi_1) \exp(-j\beta_{TM}z)|^2 \quad (19)$$

where

$$\frac{B}{A} = \left| \frac{B}{A} \right| \exp(j\phi_1) = C \exp(j\phi_1)$$

and the voltage standing wave ratio will be given by

$$R = \left( \frac{I_{\max}}{I_{\min}} \right)^{\frac{1}{2}} = \frac{1+C}{1-C} \quad (20)$$

or

$$C = \frac{R-1}{R+1}.$$

The distance between successive minima is

$$l = \frac{2\pi}{\beta_{TE} - \beta_{TM}} = \frac{\lambda_{\sigma TE} \cdot \lambda_{\sigma TM}}{\lambda_{\sigma TM} - \lambda_{\sigma TE}}. \quad (21)$$

Since there is no longitudinal wall-current flow at  $\varphi = 0$  for the two modes, a slot and moving probe can be used, and the quantity  $C$  can be determined from the measured standing wave ratio  $R$ . It is also fairly easy to determine mode purity, i.e., the presence of higher order modes other than the  $TM_{11}$  mode, by plotting the probe-current distribution

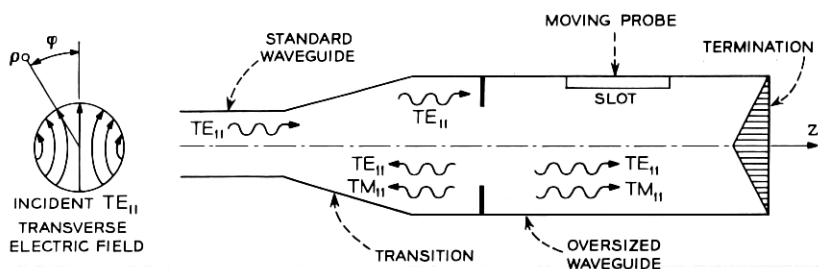


Fig. 11 — Measurement of conversion coefficient.

curve as we move between two minima. The harmonic variation of detector current with a periodicity given by (19) will be distorted if more than two modes are present.

This method of measurement requires that unidirectional traveling waves be present for the two modes, with no waves reflected from the termination. With a fairly extended load at the end of the oversized waveguide, a voltage reflection coefficient at the termination of less than 0.01 was obtained over a wide frequency band.

A practical limiting factor appeared when measuring mode content at frequencies that were far from the  $TM_{11}$  mode cut-off. As seen from (21), the minimum probe travel is proportional to  $1/(\lambda_{\theta TE} - \lambda_{\theta TM})$  which becomes very large as we move away from cut-off. In an oversized circular waveguide with 2.8" diameter and  $TM_{11}$  mode cut-off at  $f_c^{TM} = 5120$  mc, it was difficult to make measurements at frequencies higher than 6500 mc.

A block diagram of the experimental arrangements is shown in Fig. 12.

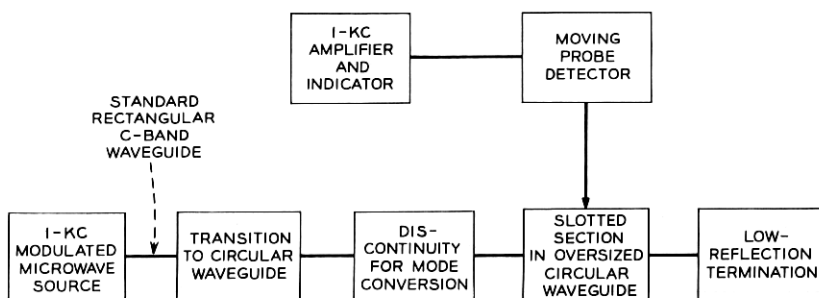


Fig. 12 — Experimental arrangement.

## IV. EXPERIMENTAL RESULTS

Measured values of mode conversion coefficient  $C$  for iris and step discontinuities are shown in Figs. 13–17. The highly dispersive character of the transition-iris combination is evident in Fig. 13. The transition used was a standard transition from TD-2 rectangular waveguide to 2.8" I.D. circular waveguide. A 12" section of 2.8" I.D. circular waveguide was placed between the iris and transition. A backward traveling  $TM_{11}$  wave is totally reflected at the transition between standard and oversized waveguides and is recombined with the forward traveling  $TM_{11}$  wave. The peak values correspond to points of positive interference, with amplitude  $2C_0$  in (12). At the higher frequencies, the  $TE_{31}$  and higher order modes were observed whenever the backward traveling  $TM_{11}$  wave was reflected from a noncircular portion of the transition.

In Fig. 14, values of mode conversion are measured for different iris sizes at a frequency range where the reflected  $TM_{11}$  wave combines with the forward wave to give the peak value of conversion coefficient  $C =$

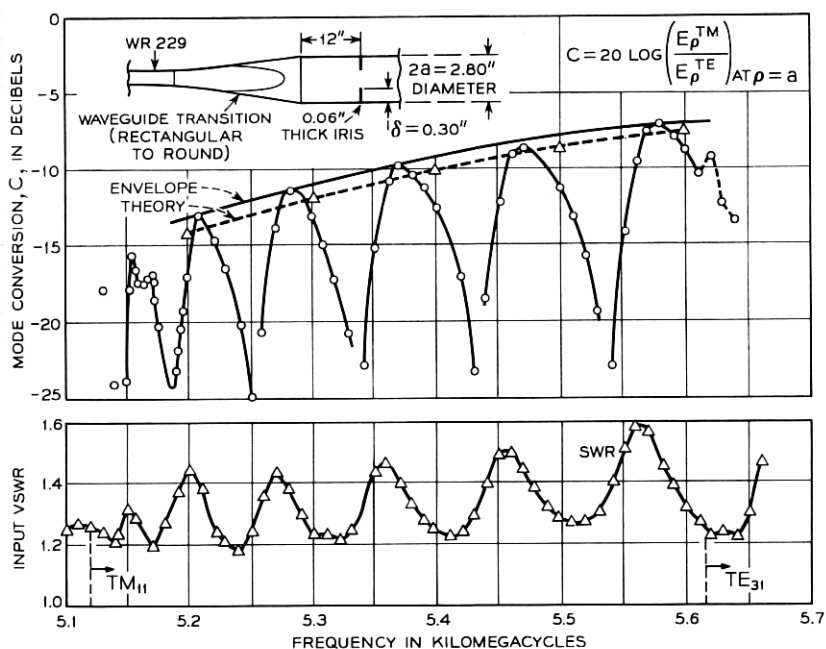


Fig. 13—Mode conversion for transition-iris coupler, compared with quasi-static approximation.

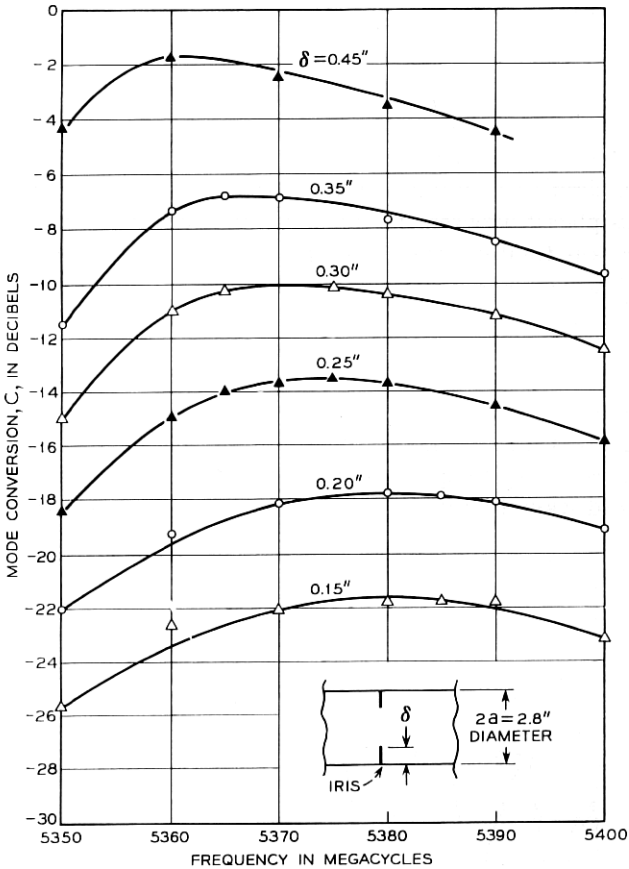


Fig. 14 — Mode conversion for transition-iris coupler.

$2C_0$ . The derived values of  $C$  as a function of frequency, with the iris size as parameter, are shown in Fig. 15. The values are compared with the quasi-static approximation of (12). The overall reflection, measured in the standard  $C$ -band waveguide preceding the transition, is also shown. The theoretical approximation is seen to give good results, especially for the smaller discontinuities, where  $\delta/a < 0.25$ . The power reflected at the iris is then less than 0.05 of the incident power.

In Fig. 16, measured values of mode conversion are given for a step discontinuity. The waveguide to the left of the step is below cut-off for the  $TM_{11}$  wave. The mode conversion under these conditions is flat over

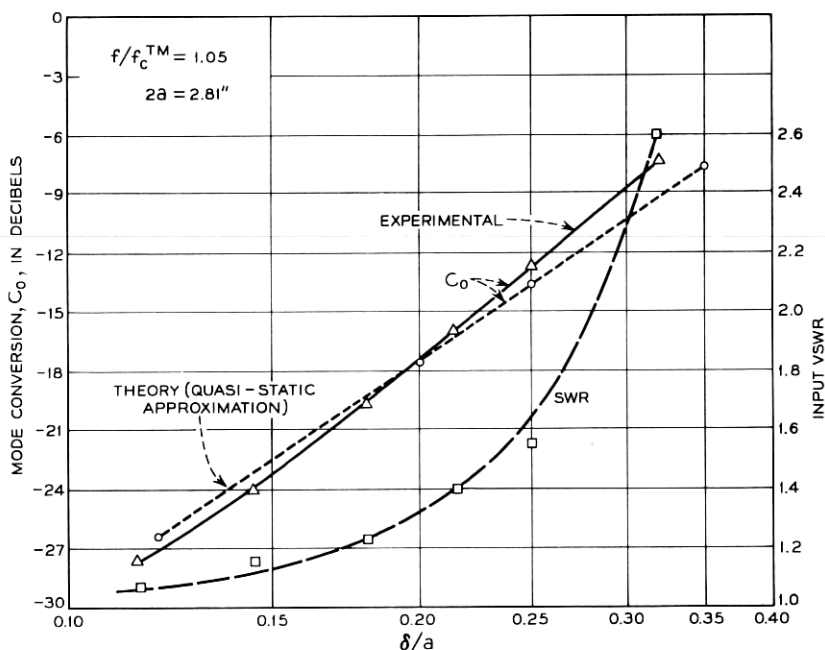


Fig. 15— Mode conversion and overall input SWR for iris, (no reflected wave from transition).

a very wide range of frequencies. In the upper curve in Fig. 16, measured values of mode conversion are given for a step in combination with an iris, again resulting in a flat frequency response. The step-iris combination provides a means for making fine adjustments of mode conversion above the value provided by the step alone.

In Fig. 17, mode conversion at a step is plotted as a function of step size. It is of interest to note the linear dependence of  $C$  on step size, which bears out the prediction made by the theoretical approximation. The incident power reflection was small for step discontinuities, being less than  $-17$  db in all cases, and less than  $-28$  db for all steps measured at 6000 mc.

## V. CONCLUSIONS

Any discontinuity in a circular waveguide which distorts the  $TE_{11}$  mode in such a way as to introduce a longitudinal component of electric field will couple the  $TE_{11}$  and  $TM_{11}$  modes of propagation. Prevention of

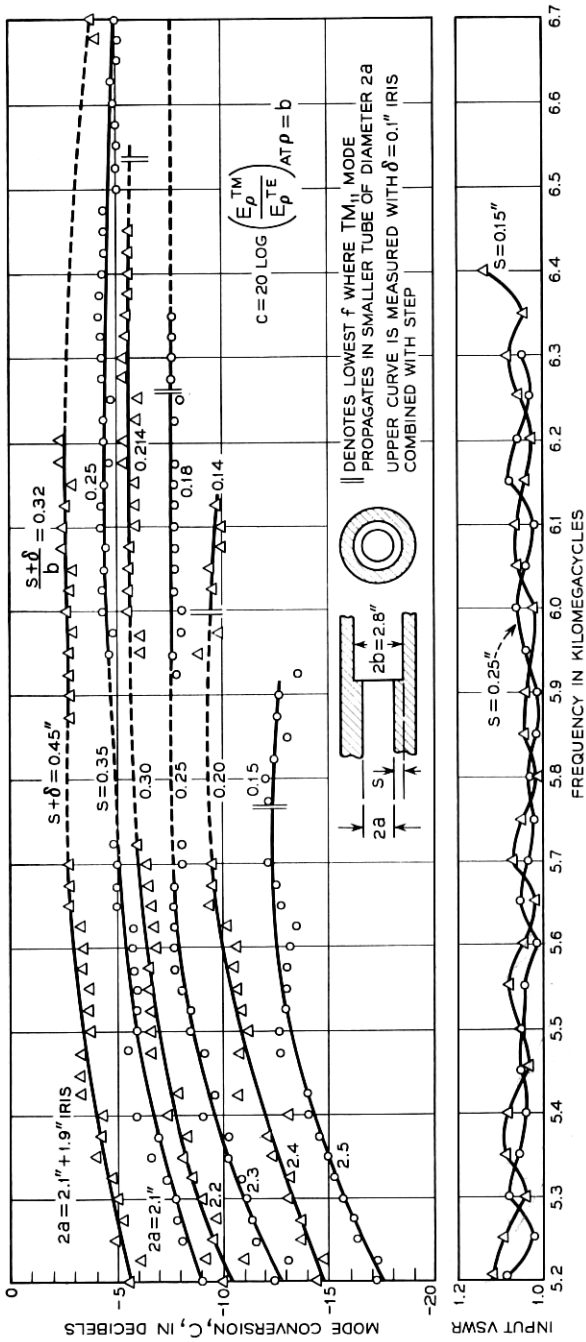


Fig. 16 — Mode conversion at step discontinuity in circular waveguide.



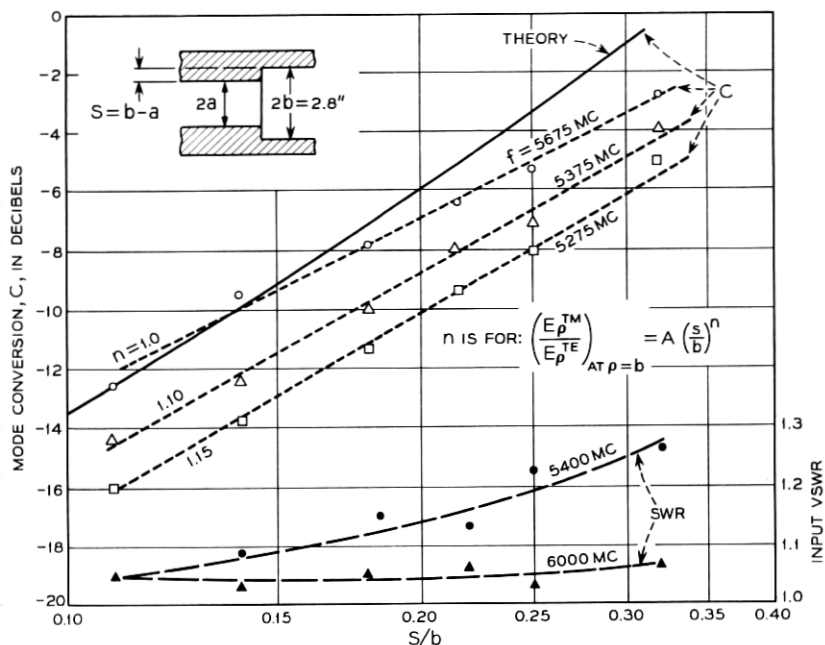


Fig. 17 — Mode conversion at step discontinuity.

coupling between these and other modes can be controlled by maintaining circular symmetry in the discontinuity and limiting the diameter of the waveguide. Two of the simplest configurations, the iris and the step, have been evaluated here and shown to have useful characteristics.

The iris was evaluated experimentally in conjunction with a waveguide transition, but the characteristics of the iris itself have been deduced and expressed in (12) and Fig. 15.

The bidirectional and reflective character of a single iris coupler (neglecting the transition) is not unlike that of a single hole coupling two waveguides. In fact, an analogy can be drawn between a single iris coupler and a single hole coupling two waveguides whose cutoff frequencies correspond with those of the  $TE_{11}$  and  $TM_{11}$  modes in the circular guide. The theory of iteratively and continuously coupled transmission lines may be used to design couplers consisting of multiple irises. Selective loading of the modes in the circular guide can provide a further control of the distributed iris coupling characteristics.

The very low-reflection and broadband coupling characteristics of the simple step converter make it particularly useful as a means for provid-

ing mode conversion. A fine adjustment of the conversion coefficient can be made by adding an iris at the step as indicated in Fig. 16.

These conversion techniques, as presented here or appropriately extended and combined, provide the means for achieving a wide range of characteristics.

#### ACKNOWLEDGMENTS

The authors wish to thank J. S. Cook and H. Zucker for many helpful suggestions. Also acknowledged are the efforts of J. R. Donnell and R. E. Pratt, who participated in the measurements, and E. M. Elam, who helped design the measuring apparatus.

#### REFERENCES

1. Potter, P. D., A New Horn Antenna with Suppressed Side-lobes and Equal Beamwidths, *Microwave J.*, 6, 1963, p. 71.
2. Cook, J. S., Elam, E. M., and Zucker, H., The Open Cassegrain Antenna: Part I. Electromagnetic Design and Analysis, *B.S.T.J.*, this issue, pp. 1255-1300.